

Recovery of Alcohols from Water Using Polydimethylsiloxane–Silica Nanocomposite Membranes: Characterization and Pervaporation Performance

Yaser Shirazi,¹ Ali Ghadimi,¹ Toraj Mohammadi²

¹Research Centre for Membrane Separation Processes, Iran University of Science and Technology (IUST), Narmak, Tehran, Iran

²Department of Chemical Engineering, South Tehran Branch, Islamic Azad University, P.O. Box 11365-4435, Tehran, Iran

Received 19 June 2011; accepted 19 July 2011

DOI 10.1002/app.35313

Published online 3 November 2011 in Wiley Online Library (wileyonlinelibrary.com).

ABSTRACT: Different polydimethylsiloxane (PDMS) nanocomposite membranes were synthesized by incorporating various contents of nanosized silica particles to improve the PDMS pervaporation (PV) performance. A uniform dispersion of silica nanoparticles in the PDMS membranes was obtained. The nanocomposite membranes were characterized morphologically by scanning electron microscopy (SEM) and atomic force microscopy (AFM). The results showed that surface roughness increases by incorporating silica, and this decreases absorption of penetrants on the membrane. Swelling studies showed that the presence of silica nanoparticles into the PDMS membranes decreases degree of swelling, which can be attributed to rigidification of the PDMS matrix. Additionally, the results revealed that helium permeability decreases through the nanocomposite membranes, due to the more polymer chains packing. Effects of silica on recovery of isopropanol (IPA) from water mixtures were also investigated. Based on the results, incor-

porating silica nanoparticles promotes significantly the PDMS membrane selectivity because the polymer chains are rigidified and also the polymer free volume decreases. However, permeation flux decreases as diffusion of the penetrants reduces in the presence of silica nanoparticles within the PDMS membranes. As PV performance depends on operating conditions, effects of feed composition, and temperature were also studied. Moreover, recoveries of IPA, ethanol, and methanol from water mixtures were compared using the PDMS-silica nanocomposite membranes. The results demonstrated that polarity and solubility of alcohols affect permeation flux and selectivity resulting in the higher permeation flux and selectivity for IPA. © 2011 Wiley Periodicals, Inc. *J Appl Polym Sci* 124: 2871–2882, 2012

Key words: nanocomposite PDMS membranes; silica nanoparticles; pervaporation; alcohol recovery; trimethylsilanol

INTRODUCTION

Membrane-based pervaporation (PV) is an energy-intensive method of separating liquid mixtures.^{1–3} For recovery of alcohols from water, other separation technologies such as distillation, liquid–liquid extraction, carbon adsorption, and air stripping are not applicable because of feed condition limitations, large volumes of by products, or high cost of post-treatments.⁴ Recently, PV has been considered for removal of volatile organic compounds from water mixtures because of low energy consumption, low environmental pollution, and low cost.^{4,5} The recovery of organic compounds from aqueous solutions is of great importance for both commercial and environmental aspects.⁶

For polymeric membranes, extensive research was performed to find an optimized membrane material having selective interaction with a specific component of feed mixture to maximize separation performance in terms of separation factor, permeation flux, and stability. However, performance of these membranes is strongly influenced by membrane physicochemical characteristics and also process conditions such as feed concentration and temperature.^{7,8}

Separation of alcohol/water mixtures by PV is important for obtaining liquid fuels from biomass sources.⁹ The PV performance of aqueous alcohol solutions was investigated by many researchers. Shaban et al.,¹⁰ Raisi et al.,⁴ Mohammadi et al.,⁹ Han et al.,¹¹ and others investigated separation of alcohols from aqueous mixtures using different organic hydrophobic membranes. Various hydrophobic membranes have already been used for selective separation of alcohols from aqueous mixtures such as sulfonated poly(ether ether ketone),¹² G-OM-010, and 1060-SULZER.¹³ Among them, silicone containing polymers have generally been found to exhibit good

Correspondence to: T. Mohammadi (torajmohammadi@iust.ac.ir).

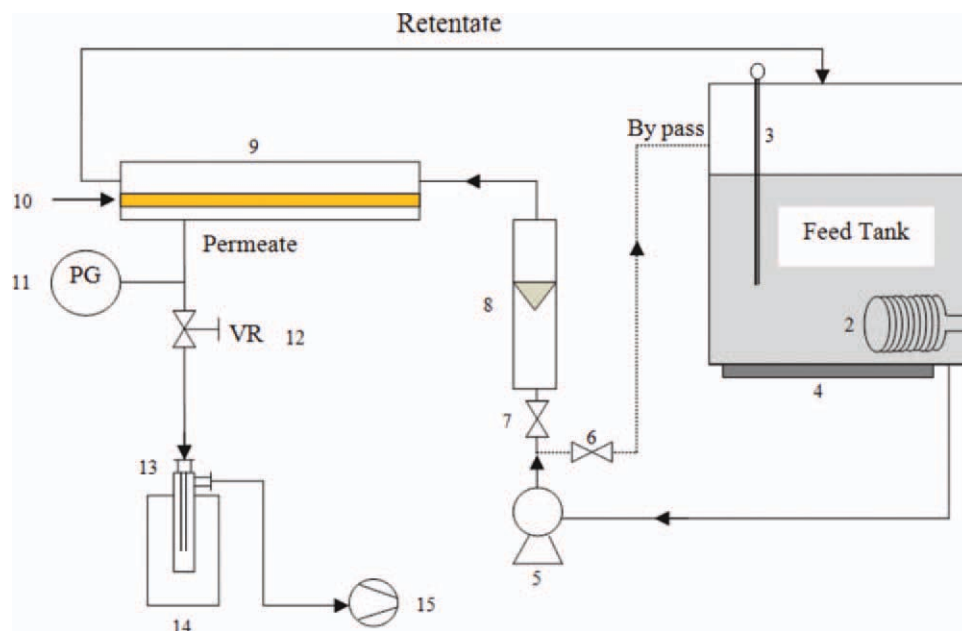


Figure 1 Schematic diagram of the PV apparatus: (1) feed tank; (2) cooling coil; (3) thermo couple; (4) heater; (5) feed pump; (6,7) valve; (8) rotor flow meter; (9) membrane cell; (10) membrane; (11) pressure gage; (12) vacuum regulator; (13) permeate collection trap; (14) liquid nitrogen trap; and (15) vacuum pump. [Color figure can be viewed in the online issue, which is available at wileyonlinelibrary.com.]

very sharp razor. The resulting films were transparent, but less than the pristine PDMS films and not tacky. Thickness of the films was determined with a digital micrometer (Mitutoyo Model MDC-25SB) readable to $\pm 1 \mu\text{m}$ and found to be approximately $250 \mu\text{m}$. In the synthesized nanocomposite membranes, PDMS-X, X; the mass ratio of TMS-H-silica over PDMS was varied at 0, 0.5, 1, 1.5, 2, 2.5, and 3. For instance: PDMS-0 is referred to the pristine PDMS and PDMS-3 is referred to the 3 wt % TMS-H-silica incorporated PDMS nanocomposite membrane.

Swelling studies

Sorption experiments were performed to study the extent of membrane swelling. These experiments are helpful to determine the interactions of membranes with liquid penetrants. Swelling experiments were performed at 30°C , gravimetrically in 1–10 wt % alcohol containing feed mixtures. The PDMS-X nanocomposite membranes were dried completely at 60°C for 8 h and weighed. Then, the nanocomposite membranes were immersed in the alcohol–water mixtures in a sealed vessel at a desired temperature for 48 h to allow them to reach the equilibrium swelling. The swollen membranes were weighed using a digital microbalance (Sartorius, TE214S) sensitive to $\pm 0.1 \text{ mg}$, as quickly as possible after wiped with tissue papers. Each run was performed at least three times, and the results were averaged. The degree of

swelling (DS) of the membranes was calculated using the following equation:

$$\text{DS} (\%) = \left(\frac{W_s - W_d}{W_d} \right) \times 100 \quad (1)$$

where W_s and W_d are mass of the swollen and the dried membranes, respectively.

PV experiments

The synthesized membranes were evaluated in PV separation using a setup as shown in Figure 1. The feed solution was circulated by a pump (Talow magnet pump, Rom, Italy) through the membrane cell. The down-stream pressure was maintained at about 1 mbar using a vacuum pump (Vac Torr 25, Houston, Texas, USA), while the feed pressure was atmospheric. In fact, partial vacuum was applied to the permeate side as a driving force for alcohols to evaporate easily. The permeate vapor was collected in a cold trap (liquid nitrogen) to be condensated. The collected permeate sample was weighted to determine the permeation flux. The concentrations of feed and permeate were measured using gas chromatography (Tehran, Iran) provided with a thermal conductivity detector equipped with a DEGS or Tenax packed column of 1/8 in. internal diameter (i.d.), internal diameter, having 2 m length. The GC response was calibrated for the column and known compositions of different alcohol–water mixtures.

Permeation properties of the membranes were characterized by PV selectivity (α_{PV}), total permeation flux (J_P), and PV separation index (PSI) using the following equations, respectively:

$$\alpha_{PV} = \frac{y_A/y_B}{x_A/x_B} \quad (2)$$

$$J_P = \frac{W_P}{At} \quad (3)$$

$$PSI = J_P(\alpha_{PV} - 1) \quad (4)$$

where y_A and y_B are mass fractions of alcohol and water in the permeate, respectively, and x_A and x_B are mass fractions of alcohol and water in the feed, respectively. The permeation flux, J_P ($\text{kg}/\text{m}^2 \text{ h}$), was calculated using W_P , the permeate mass (kg), A , the effective membrane area (m^2), and t , the permeation time (h).

RESULTS AND DISCUSSION

Characterization of PDMS-X nanocomposite membranes

SEM observation

To investigate the dispersion of TMS-H-silica nanoparticles in the PDMS membranes, SEM characterization of the 2 and 3 wt % TMS-H-silica incorporated PDMS membranes was carried out. As shown in Figure 2, TMS-H-silica incorporated PDMS membranes are dense with no macroscopic voids and TMS-H-silica nanoparticles are dispersed uniformly within the PDMS matrix. The TMS-H-silica nanoparticles adhere well to the PDMS due to the high compatibility between the TMS-H-silica nanoparticles and the hydrophobic PDMS.

AFM analysis

Different PDMS-X nanocomposite membranes were synthesized under similar preparation conditions and their roughnesses as well as particle distribution were compared. According to the AFM images (Fig. 3), it was found out that TMS-H-silica nanoparticles are appropriately dispersed over the surface of PDMS membranes. Table 1 presents the surface roughness of various PDMS-X nanocomposite membranes. As observed, the surface roughness of the PDMS-X nanocomposite membranes increases by introducing more amounts of TMS-H-silica nanoparticles into the polymer matrix. As a result, the pristine PDMS and the PDMS-3 nanocomposite membrane are the smoothest and the roughest membranes, respectively.

Additionally, it should be mentioned that in organic-inorganic nanocomposite membranes, the

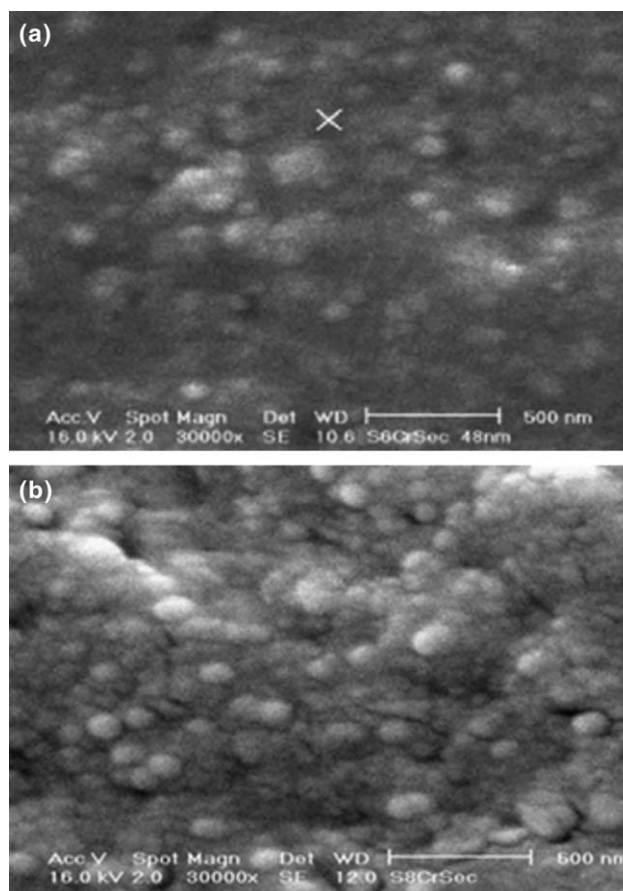


Figure 2 SEM cross-section image of nanocomposite membranes (a) PDMS-2 and (b) PDMS-3.

tendency to agglomeration increases at higher filler content and this may distort the performance of nanocomposite membranes by formation of nonselective voids. However, it is impossible to completely detect presence of these voids between the polymer matrix and the nanoparticles, by AFM and SEM images.

Verification of nonselective voids: Helium permeation test

To verify compatibility of TMS-H-silica nanoparticles with PDMS matrix and investigate the presence of nonselective voids in the PDMS-X nanocomposite membranes, permeability of Helium through various PDMS-X nanocomposite membranes were measured at two different pressure gradients (1 and 6 atm).

Because of its small size, Helium serves as an excellent probing gas for identifying the presence of voids.³² The presence of nonselective voids into the PDMS-X nanocomposite membranes at the interface of polymer and TMS-H-silica nanoparticles can offer high permeable sites for Helium because of its diminutive size. Permeability values of Helium through the PDMS-X nanocomposite membranes are

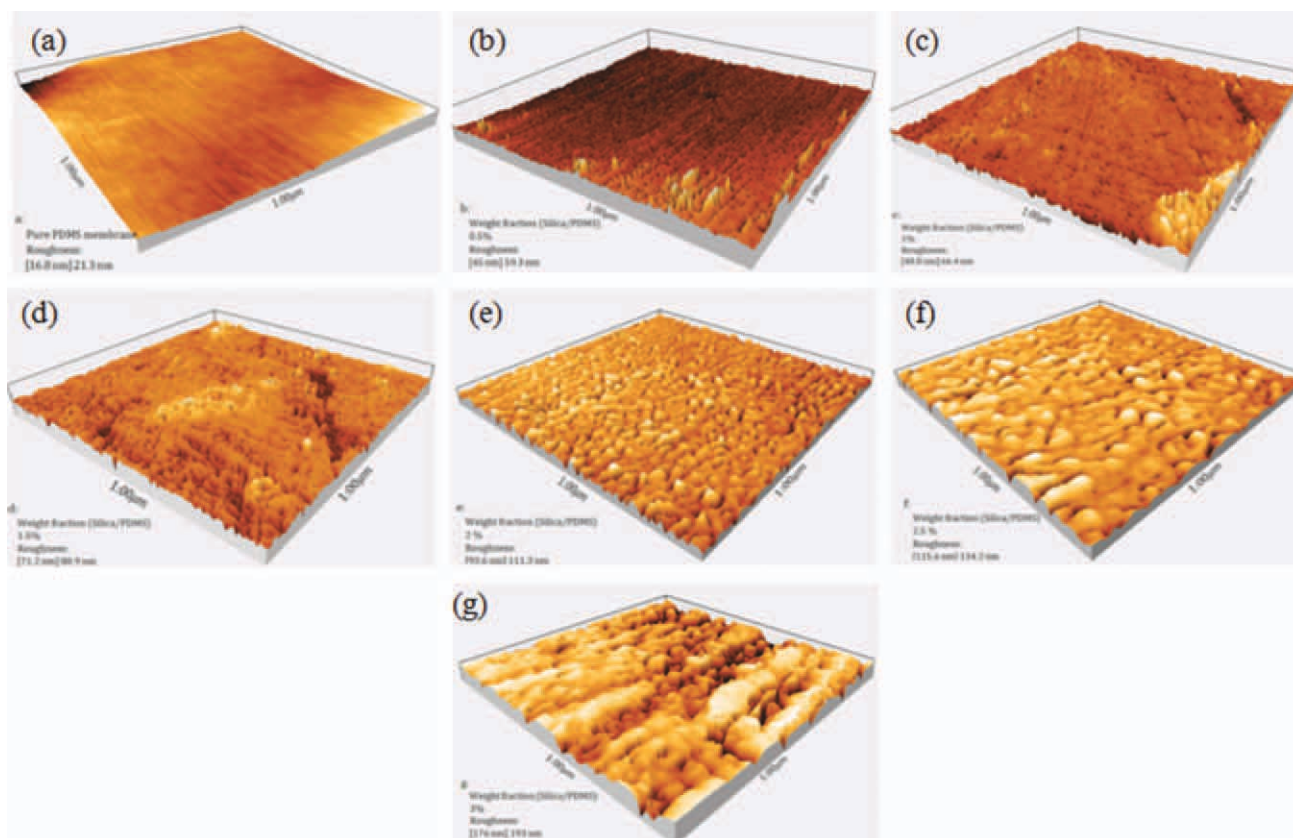


Figure 3 AFM 3D images of nanocomposite membranes: (a) PDMS-0, (b) PDMS-0.5, (c) PDMS-1, (d) PDMS-1.5, (e) PDMS-2, (f) PDMS-2.5, and (g) PDMS-3. [Color figure can be viewed in the online issue, which is available at wileyonlinelibrary.com.]

presented in Table 2. It is completely evident that permeability of Helium decreases with increasing TMS-H-silica nanoparticles content in the PDMS matrix. This behavior suggests that the PDMS polymer adheres well to the TMS-H-silica nanoparticles. Hence, it can be concluded that the synthesized PDMS-X nanocomposite membranes are defect free. Furthermore, reduction of Helium permeability values of the PDMS membranes in the presence of TMS-H-silica nanoparticles also suggests that the silica makes the polymer chains rigid.

Swelling of PDMS-X nanocomposite membranes for IPA-water mixtures

DS of the PDMS-X nanocomposite membranes in 4 wt % IPA in water mixture at 30°C is illustrated in

Figure 4. As observed, the pristine PDMS membrane shows higher swelling compared with the PDMS-X nanocomposite membranes. This can be due to the presence of TMS-H-silica nanoparticles into the polymer matrix, which decreases absorption of IPA into the membrane. As mentioned, incorporating the TMS-H-silica increases the membrane surface roughness. The membrane surface properties can influence the absorption of penetrants. This phenomenon causes penetrants in the feed side hardly absorb on the membrane surface. Furthermore, increasing the membrane surface roughness increases the membrane contact angle. Hyder et al.⁷ indicated that a membrane with higher surface roughness shows higher contact angle. As a result, the pristine PDMS membrane with the lowest surface roughness exhibits the highest DS, and on the other hand, the

TABLE I
Surface Roughness of Different PDMS-X Nanocomposite Membranes

Roughness	Membrane						
	PDMS-0	PDMS-0.5	PDMS-1	PDMS-1.5	PDMS-2	PDMS-2.5	PDMS-3
Average (nm)	16.8	45	48.8	71.2	93.6	116.6	176
Maximum(nm)	23.1	59.3	66.4	80.9	111.3	134.2	193

TABLE II
Permeability of Helium Through Different PDMS-X Nanocomposite Membranes

ΔP (atm)	Membrane						
	PDMS-0	PDMS-0.5	PDMS-1	PDMS-1.5	PDMS-2	PDMS-2.5	PDMS-3
1	723 \pm 3	694 \pm 7	663 \pm 9	632 \pm 8	606 \pm 6	567 \pm 8	528 \pm 7
6	611 \pm 4	595 \pm 9	573 \pm 4	549 \pm 7	523 \pm 10	507 \pm 3	486 \pm 5

The unite of permeability = Barrer

PDMS-3 nanocomposite membrane with the highest surface roughness exhibits the lowest DS.

Furthermore, DS reduction also suggests that PDMS becomes rigid after incorporating TMS-H-silica, giving a membrane swelling reduction, which in turn decreases the diffusive trends of penetrants through the membrane. These results are consistent with those of Helium permeability.

PV results of PDMS-X nanocomposite membranes

In this section, PV results of different PDMS-X nanocomposite membranes are investigated for separation of IPA-water mixtures. Afterward, the optimum PDMS-X nanocomposite membrane is selected for separation of different alcohol-water mixtures.

Effect of silica content on PV performance

Effects of the TMS-H-silica content on selectivity and permeation flux of the PDMS membranes are presented in Figure 5. As shown, permeation flux decreases with increasing the TMS-H-silica content. This can be due to the fact that distribution of the TMS-H-silica nanoparticles in the membrane increases transport resistance of both IPA and water molecules; therefore, permeation flux of the PDMS-X nanocomposite membranes are less than that of the pristine PDMS membrane. On the other hand, presence of the TMS-H-silica nanoparticles in the poly-

mer matrix can increase the membrane pathway and also decrease diffusion of penetrants through the membrane. It must be mentioned that, the pristine PDMS membrane with the highest DS also exhibits the highest permeation flux. Obviously, the permeation flux values of different PDMS-X nanocomposite membranes follow a similar trend with the swelling results. This means that the membranes with higher DS, exhibit higher permeation flux. However, it is observed that with increasing the TMS-H-silica content in the polymer matrix, the membrane selectivity increases. This can be attributed to higher packing of the PDMS chains due to the presence of TMS-H-silica nanoparticles. Moreover, the polymer chains packing can reduce the polymer free volume, and this results in higher selectivity and less permeation flux.^{1,33} In addition, as silica has negligible sorption capacity, it can act as a physical crosslinker for PDMS.³⁴ The more crosslinked PDMS is known to lead to higher selectivity and less permeation flux due to its higher resistance against the swelling by solvent sorption.³⁴⁻³⁶

Effect of feed composition on PV performance

PV performance of the PDMS membranes depends upon the composition of feed mixtures.³⁷ Selectivity and permeation flux of various PDMS-X nanocomposite membranes using 1–10 wt % IPA in water mixtures and at feed temperature of 30°C are

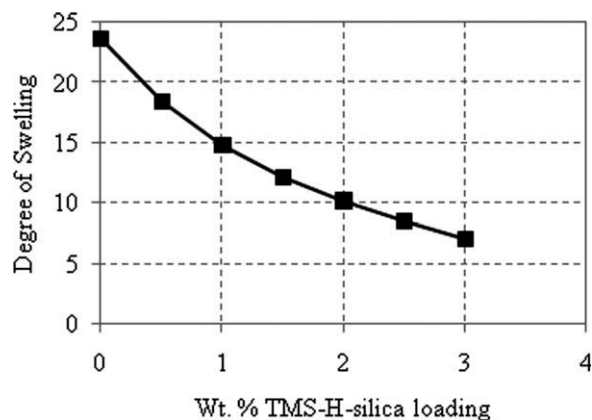


Figure 4 DS of different PDMS-X nanocomposite membranes in the 4 wt % IPA in water mixture at 30°C.

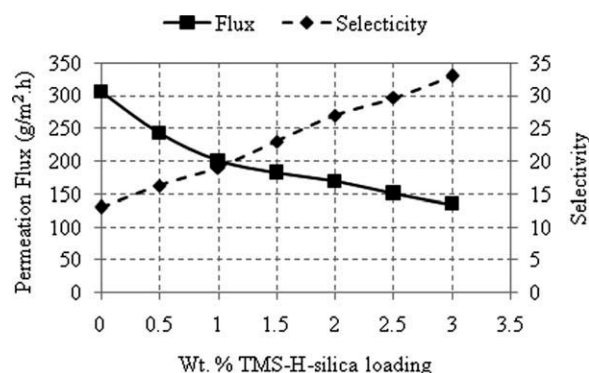


Figure 5 Effect of TMS-H-silica loading on PV performance of the PDMS-X nanocomposite membranes in the 4 wt % IPA in water mixture at 30°C.

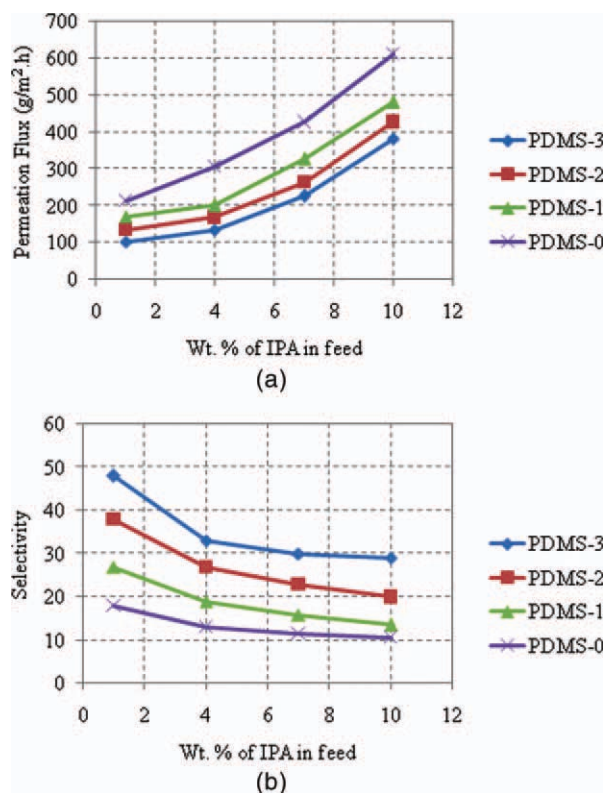


Figure 6 Effect of wt % of IPA in feed on (a) permeation flux (b) IPA selectivity of different PDMS-X nanocomposite membranes. [Color figure can be viewed in the online issue, which is available at wileyonlinelibrary.com.]

presented in Figure 6. As observed, permeation flux increases as IPA content in the feed increases, and this is mostly due to the membrane swelling. The swollen polymer exhibits less resistance against permeation of penetrants due to the more space between its chains.^{9,17} Increasing IPA content in the feed enhances interactions of the membrane with the penetrants, and this results in higher permeability of penetrants through the membrane. In other words, higher concentration of IPA in the feed mixture causes the amorphous region of membrane to swell, and thus the polymer chains to become flexible, and enhances diffusion of the penetrants. Although, increasing IPA concentration in the feed mixture favors permeation of permeating molecules, the membrane selectivity decreases due to easier diffusion of water molecules through the swollen polymer matrix.

Additionally, increasing IPA concentration in the feed mixture increases free volume of the membrane and simultaneously mobility of side chains increases. Consequently, smaller water molecules can permeate more easily through the membrane. In other words, this phenomenon enhances permeation of water through the membrane and as a result the membrane selectivity decreases.

A comparison of different PDMS-X nanocomposite membranes exhibits that the PDMS-3 nanocomposite membrane has higher selectivity even at high IPA content in the feed. This can be explained by the less swelling of the PDMS-3 nanocomposite membrane at high IPA content.

Effect of feed temperature on PV performance

PV process is known to be temperature dependent as both permeation flux and selectivity are influenced by changing temperature.¹⁷ Figure 7 illustrates effects of feed temperature on PV performance of different PDMS-X nanocomposite membranes at temperature range of 30–60°C using 4 wt % IPA in water mixture. With increasing the feed temperature, vapor pressures of both IPA and water in the feed side enhance; however, these values in the permeate side are constant. As driving force for permeation is concentration gradient, resulting from the difference in partial vapor pressure of penetrates between feed and permeate mixtures, increasing vapor pressure, which favors transport of penetrants through the membrane, enhances permeation flux. In addition, increasing feed temperature enhances thermal mobility of the polymer chains, and this generates extra free volume within the polymer matrix, and

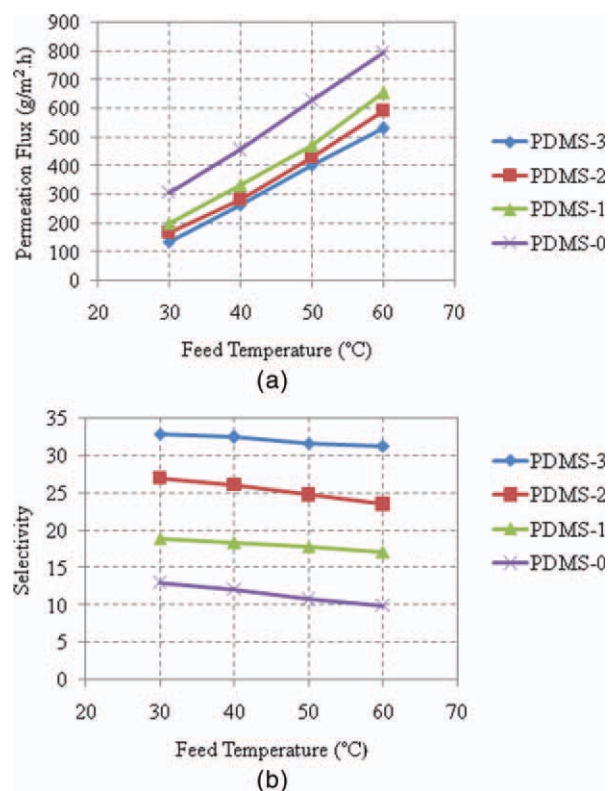


Figure 7 Effect of feed temperature on (a) permeation flux (b) IPA selectivity of different PDMS-X nanocomposite membranes. [Color figure can be viewed in the online issue, which is available at wileyonlinelibrary.com.]

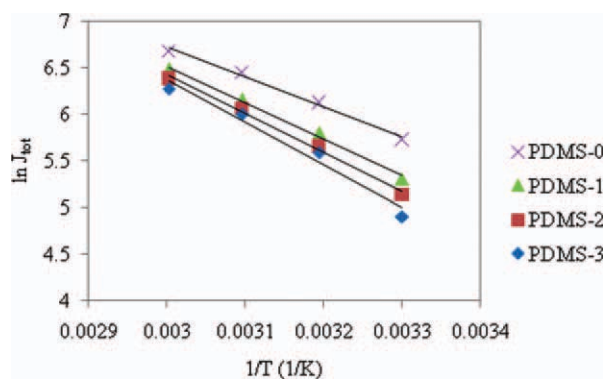


Figure 8 $\ln J_{\text{tot}}$ versus $1/T$ for different PDMS-X nanocomposite membranes. [Color figure can be viewed in the online issue, which is available at wileyonlinelibrary.com.]

consequently promotes the sorption and diffusion rates of permeating compounds.³⁸ This also enhances the plasticization effect in the polymer segments and facilitates transport of water molecules through the membrane, and thus reduces the membrane selectivity.³⁹

Moreover, theoretical diffusivity of the permeating molecules increases exponentially as temperature increases, and this results in higher permeation flux.⁴⁰ It must be mentioned that increasing feed temperature increases the amorphous region in the polymer matrix, and smaller molecules (with larger diffusion coefficient) can permeate more readily than larger molecules. In this case, as molecular size of water is smaller than that of IPA, it can pass easier than IPA through the membrane with increasing feed temperature and this phenomenon decreases the PDMS membranes selectivity.

Temperature dependency of permeation flux for permeating components (J_i) can be studied by the Arrhenius type relation as follows:

$$J_i = J_{i_0} \exp\left(\frac{-E_{pi}}{RT}\right) \quad (5)$$

where J_{i_0} is the Arrhenius constant, E_{pi} is the activation energy of permeating components, R is the universal gas constant, and T is the feed temperature.

The Arrhenius plots of $\ln J_{\text{tot}}$ versus $1/T$ for the PDMS-X nanocomposite membranes are shown in Figure 8. Activation energy values of various PDMS-X nanocomposite membranes were calculated from the slopes of these Arrhenius plots. The linear relationship observed suggests that the temperature dependency of permeation flux obeys the Arrhenius relationship.

Activation energy values of the PDMS-0, PDMS-1, PDMS-2, and PDMS-3 nanocomposite membranes are 26.8, 32.7, 35.2, and 38.1 (kJ/mol), respectively.

As observed, the values of activation energy for all the PDMS-X nanocomposite membranes are positive. This indicates that permeation flux values of permeating components increase with increasing feed temperature. Furthermore, activation energy values of the nanocomposite membranes increase when more TMS-H-silica is incorporated to the PDMS membrane. This also indicates that diffusion of penetrants through the nanocomposite membranes decreases by incorporating TMS-H-silica to the PDMS membrane and confirms the permeation flux reduction through the PDMS-X nanocomposite membranes. The results show that the higher activation energy, the higher membrane selectivity.

PSI values of different PDMS-X nanocomposite membranes

PSI value which is the product of permeation flux and membrane selectivity has been widely used to evaluate the overall PV membrane performance. The results are presented in Figure 9. As observed, the PSI values do not change from PDMS-0 to PDMS-1 nanocomposite membranes. This is due to the fact that the higher membrane selectivity is compensated with the lower permeation flux for the PDMS-1 nanocomposite membrane. However, by increasing TMS-H-silica content, the membrane selectivity increases more significantly and this much higher membrane selectivity is not compensated with the lower permeation flux, and thus the PSI values increases.

Recovery of IPA from water using different PDMS-X nanocomposite membranes indicated that the PDMS-3 nanocomposite membrane exhibits the higher PV performance compared with the other PDMS-X nanocomposite membranes. Therefore, the PDMS-3 nanocomposite membrane was selected for further investigation of the PV separation performance of different alcohol–water mixtures.

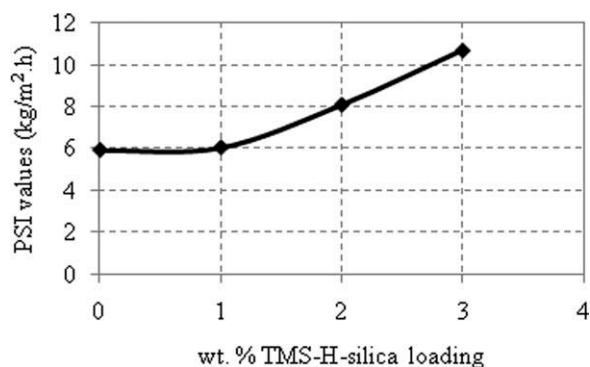


Figure 9 Effect of TMS-H-silica loading on PSI values of different PDMS-X nanocomposite membranes.

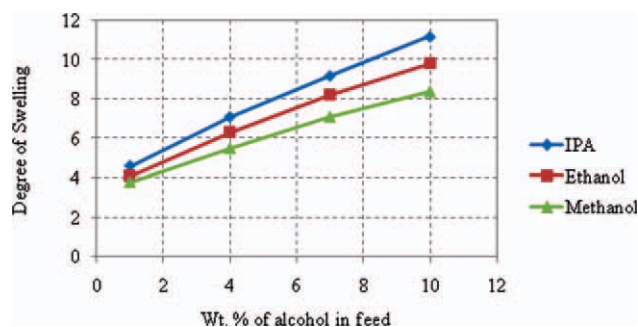


Figure 10 DS of the PDMS-3 nanocomposite membrane in different alcohol–water mixtures. [Color figure can be viewed in the online issue, which is available at wileyonlinelibrary.com.]

Comparison of PV performance for alcohol removal from different alcohol–water mixtures using the PDMS-3 nanocomposite membrane

Swelling results of different alcohol–water mixtures

Figure 10 illustrates DS of the PDMS-3 nanocomposite membrane in different alcohol–water mixtures. DS of different alcohol–water mixtures was measured as a function of alcohol concentration. The swelling measurements were carried out at feed temperature of 30°C using alcohol 1–10 wt % in

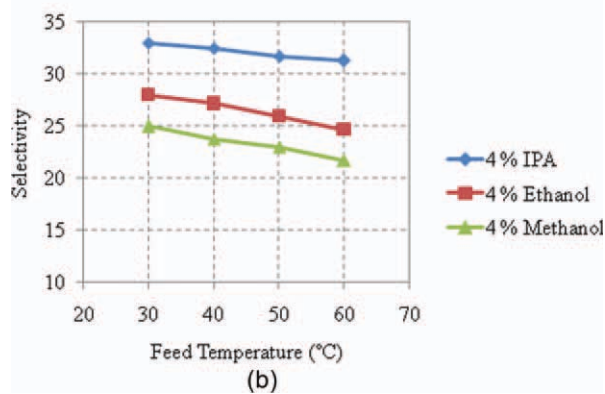
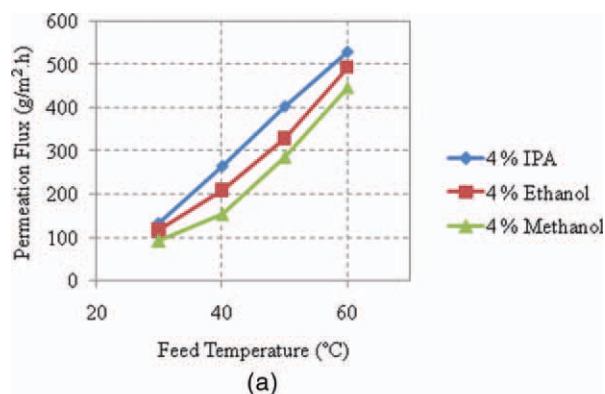


Figure 12 Effect of feed temperature on (a) permeation flux (b) IPA selectivity of different alcohol–water mixtures. [Color figure can be viewed in the online issue, which is available at wileyonlinelibrary.com.]

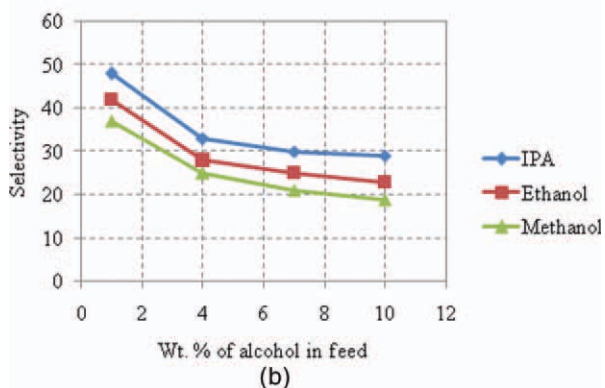
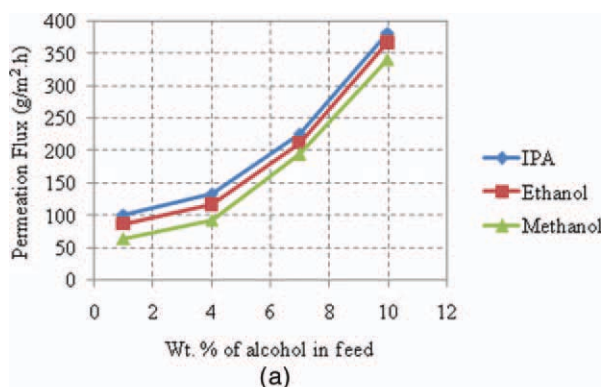


Figure 11 Effect of wt % of alcohols in feed on (a) permeation flux (b) IPA selectivity of different alcohol–water mixtures. [Color figure can be viewed in the online issue, which is available at wileyonlinelibrary.com.]

water mixtures. As observed, DS values in IPA–water mixtures are higher than those in ethanol–water and methanol–water mixtures. This can be attributed to solubility parameter difference of IPA ($23.6 \text{ (J/cm}^3)^{1/2}$), ethanol ($26.2 \text{ (J/cm}^3)^{1/2}$), and methanol ($29.7 \text{ (J/cm}^3)^{1/2}$) with PDMS ($14.9 \text{ (J/cm}^3)^{1/2}$) membrane.^{9,41} In other words, the less solubility parameter difference between IPA and PDMS membrane means that IPA molecules absorb into the membrane more easily compared with ethanol and methanol.

Effects of feed composition on PV performance of the PDMS-3 nanocomposite membrane using different alcohol–water mixtures

Figure 11 presents permeation flux and selectivity of the PDMS-3 nanocomposite membrane using different alcohol–water mixtures, at feed temperature of 30°C, using 1–10 wt % alcohol in water mixture. As observed, IPA and methanol have higher and lower permeability, respectively. The trend of selectivity is also similar to that of permeation flux. Generally, permeation of molecules through a dense polymer matrix is governed by the solution–diffusion mechanism, based on that, the components dissolve in the

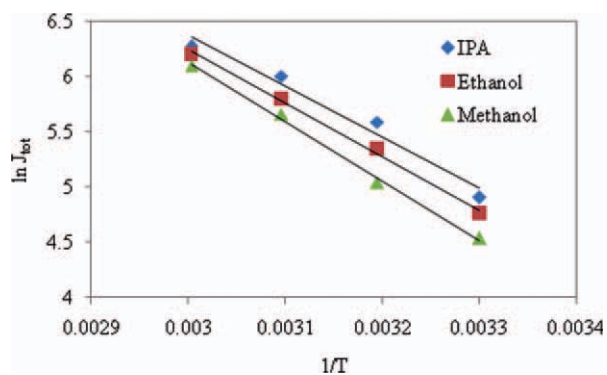


Figure 13 $\ln J_{\text{tot}}$ versus $1/T$ for different alcohol–water mixtures. [Color figure can be viewed in the online issue, which is available at wileyonlinelibrary.com.]

polymer and diffuse to the downstream side of the membrane. Therefore, solubility and diffusivity of permeants through the membrane control permeation flux and selectivity. As mentioned, solubility parameter of PDMS is closer to that of IPA than those of ethanol and methanol,^{9,41} then, the PDMS membrane is more selective to IPA compared with ethanol and methanol. Solubility parameter is a measure of affinity between polymer and solvent. As the affinity between solvent and polymer enhances, the more solvent is absorbed inside the polymer and consequently permeation flux increases.⁴¹

It can be also said that permeability of hydrophobic membranes toward aliphatic alcohols involves transfer of polar molecules (the alcohols) through nonpolar environments (the membranes). Increasing molecular weight of alcohols decreases their polarity, favoring the membrane permeability.⁴² As a matter of fact, the molecular polarity decreases from methanol to IPA, and the interaction between alcohol molecules and the polymer chains decreases from methanol to IPA. Therefore, IPA molecules are more likely to diffuse in the

PDMS-3 nanocomposite membrane compared with ethanol and methanol.

Effects of feed temperature on PV performance of the PDMS-3 nanocomposite membrane using different alcohol–water mixtures

Figure 12 illustrates effects of feed temperature on PV performance of the PDMS-3 nanocomposite membrane for removal of different alcohols from aqueous solutions. As seen, for all the studied alcohols (IPA, ethanol, and methanol)-water mixtures increasing feed temperature promotes permeation flux and diminished the membrane selectivity. As observed, IPA-water mixtures have higher permeation flux compared with ethanol and methanol–water mixtures at all feed temperatures. Increasing feed temperature causes the amorphous region of the membrane to swell more, and thus causes the polymer chains to become more flexible and increases the membrane free volume which is available for diffusion of relatively more nonpolar molecules.⁹

Figure 13 shows that plot of the logarithm of PV permeation flux versus the reciprocal of absolute temperature are generally straight lines. This means that permeation flux data are fitted to the Arrhenius equation. The calculated activation energies for IPA, ethanol, and methanol–water mixtures are 38.15, 40.12, and 44.70 (kJ/mol), respectively. As observed, activation energy of IPA is lower than those of ethanol and methanol. This can be attributed to the fact that IPA can permeate through the PDMS-3 nanocomposite membrane more readily than the other alcohols. Additionally, it can be said that activation energy of alcohol permeation increases as difference in solubility parameter between the alcohol and the membrane increases.⁹

TABLE III
PV Separation of Alcohols-Water Mixtures Using PDMS Membranes Incorporated with Different Fillers

Membrane	T (°C)	Alcohol in feed (wt %)	Flux ($\text{g}/\text{m}^2 \text{ h}$)	Selectivity	Reference
PDMS-0	30	4 ^a	306	13	This study
PDMS-3	30	4 ^b	117	28	This study
	30	4 ^a	135	33	This study
	50	4 ^a	405	31.7	This study
	50	4 ^b	329	26	This study
PDMS-SY2	50	4.84 ^a	127	13.6	34
PDMS-ZSM5	50	4.84 ^a	132	13.3	34
PDMS-silicalite-1	22.5	5 ^b	51	16.5	29
PDMS-zeolite Y	35	– ^b	750	4.5	29
PDMS-carbon black	35	– ^b	–	9	29
PDMS-fumed silica	40	5 ^b	–	7	29
PDMS-fumed silica (A200)	40	5 ^b	200	19	29

^a Isopropanol.

^b Ethanol.

Comparison of PV performance of PDMS-filled membranes

Comparison of PV performance of PDMS membranes with different fillers for recovery of IPA and ethanol from water mixtures is listed in Table 3. According to literature, zeolites have been used frequently to improve the PV performance of PDMS membranes. As observed, zeolites mostly increase both permeability and selectivity; however, selectivity of zeolites incorporated PDMS membranes is still low. Also, fumed silica incorporated PDMS membranes exhibits higher permeability; however, due to the low compatibility of this filler with the polymer matrix, their selectivity decreases. As presented in this study, the TMS-H-silica interacts better with the PDMS matrix and rigidifies the polymer chains and this favors selectivity of the PDMS membrane.

One can observe that permeation flux of the PDMS-X nanocomposite membranes is moderate, while their selectivity is significantly higher than those of the other incorporated PDMS membranes.

CONCLUSION

Different contents of TMS-hydrophobized silica were incorporated into the PDMS membrane to synthesize the PDMS-X nanocomposite membranes. The nanocomposite membranes were characterized by SEM and AFM to investigate dispersion of the TMS-H-silica nanoparticles in the PDMS matrix and also effect of silica content on surface properties of the polymer. The results showed that incorporating the TMS-H-silica nanoparticles increases surface roughness of the membranes and thus decreases absorption of penetrants into the polymer. SEM observation revealed that the TMS-H-silica nanoparticles can interact appropriately with the PDMS matrix, without formation of nonselective voids. Additionally, Helium permeability measurements showed that incorporating the TMS-H-silica nanoparticles rigidifies the PDMS matrix. The PDMS-X nanocomposite membranes were used to remove IPA from water mixtures. Increasing the TMS-H-silica content reduces permeation flux due to the reduction of polymer free volume and the increment of pathway in the PDMS membrane. However, selectivity of the PDMS-X nanocomposite membranes increases significantly due to the higher polymer chains packing and also the less membrane swelling.

Furthermore, the PDMS-3 nanocomposite membrane was used to compare the PV performance for recovery of different alcohols from water. The results demonstrated that both permeation flux and selectivity of the PDMS-3 nanocomposite membrane for IPA-water mixtures are more than those for ethanol and methanol-water mixtures. This can be due

to the fact that IPA solubility parameter is closer to PDMS solubility parameter and also IPA is less polar. From the results, it can be concluded that the TMS-H-silica incorporated PDMS membranes can be appropriately used for recovery of alcohols from water mixtures.

Reference

- Shirazi, Y.; Tofighy, M. A.; Mohammadi, T.; Pak, A. *J Membr Sci* 2011, 378, 551.
- Shahverdi, M.; Mohammadi, T.; Pak, A. *J Appl Polym Sci* 2011, 119, 1704.
- Rezakazemi, M.; Shahverdi, M.; Shirazian, S.; Mohammadi, T.; Pak, A. *Chem Eng J* 2011, 168, 60.
- Raisi, A.; Aroujalian, A.; Kaghazchi, T. *Sep Sci Technol* 2009, 44, 3538.
- Mohammadi, T.; Kikhavandi, T.; Moghbeli, M. *J Appl Polym Sci* 2008, 107, 1917.
- Zhang, X. K.; Poojari, Y.; Drechsler, L. E.; Kuo, C. M.; Fried, J. R.; Clarson, S. J. *J Inorg Organomet Polym Mater* 2008, 18, 246.
- Hyder, M. N.; Huang, R. Y. M.; Chen, P. *J Membr Sci* 2006, 283, 281.
- Verkerk, A. W.; van Male, P.; Vorstman, M. A. G.; Keurentjes, J. T. F. *J Membr Sci* 2001, 193, 227.
- Mohammadi, T.; Aroujalian, A.; Bakhshi, A. *Chem Eng Sci* 2005, 60, 1875.
- Shaban, H. I.; Ali, S. H.; Mathew, J. *J Appl Polym Sci* 2001, 82, 3164.
- Han, X. L.; Wang, L.; Li, J. D.; Zhan, X.; Chen, J. A.; Yang, J. C. *J Appl Polym Sci* 2011, 119, 3413.
- Huang, R. Y. M.; Shao, P.; Feng, X.; Burns, C. M. *J Membr Sci* 2001, 192, 115.
- Molina, J. M.; Vatai, G.; Bekassy-Molnar, E. *Desalination* 2002, 149, 89.
- Bakhshi, A.; Mohammadi, T.; Aroujalian, A. *J Appl Polym Sci* 2008, 107, 1777.
- Vane, L. M.; Namboodiri, V. V.; Meier, R. G. *J Membr Sci* 2010, 364, 102.
- Xu, G. F.; Zhu, W. P.; Gou, P. F.; Zhu, K.; Shen, Z. Q. *Acta Polymerica Sinica* 2010, 11, 1327.
- Garg, P.; Singh, R. P.; Pandey, L. K.; Choudhary, V. *J Appl Polym Sci* 2010, 115, 1967.
- Garg, P.; Singh, R. P.; Choudhary, V. *Sep Purif Technol* 2011, 76, 407.
- Li, S. Y.; Srivastava, R.; Parnas, R. S. *J Membr Sci* 2010, 363, 287.
- Razavi, S.; Sabetghadam, A.; Mohammadi, T. *Chem Eng Res Des* 2011, 89, 148.
- Sabetghadam, A.; Mohammadi, T. *Polym Eng Sci* 2010, 50, 2392.
- Sabetghadam, A.; Mohammadi, T. *Compos Interf* 2010, 17, 223.
- Li, X. H.; Wang, S. C. *Sep Sci Technol* 1996, 31, 2867.
- Lipnizki, F.; Hausmanns, S. *Sep Sci Technol* 2004, 39, 2235.
- Yi, S. L.; Su, Y.; Wan, Y. H. *J Membr Sci* 2010, 360, 341.
- Li, L.; Xiao, Z. Y.; Zhang, Z. B.; Tan, S. J. *Chem Eng J* 2004, 97, 83.
- Li, C. L.; Huang, S. H.; Hung, W. S.; Kao, S. T.; Wang, D. M.; Jean, Y. C.; Lee, K. R.; Lai, J. Y. *J Membr Sci* 2008, 313, 68.
- Zhou, H. L.; Su, Y.; Chen, X. R.; Yi, S. L.; Wan, Y. H. *Sep Purif Technol* 2010, 75, 286.
- Peng, P.; Shi, B. L.; Lan, Y. Q. *Sep Sci Technol* 2011, 46, 420.
- Tang, X. Y.; Wang, R.; Xiao, Z. Y.; Shi, E.; Yang, J. *J Appl Polym Sci* 2007, 105, 3132.

31. Ghadimi, A.; Sadrzadeh, M.; Shahidi, K.; Mohammadi, T. *J Membr Sci* 2009, 344, 225.
32. Kim, S.; Pechar, T. W.; Marand, E. *Desalination* 2006, 192, 330.
33. Sairam, M.; Patil, M. B.; Veerapur, R. S.; Patil, S. A.; Aminabhavi, T. M. *J Membr Sci* 2006, 281, 95.
34. Yang, H.; Nguyen, Q. T.; Ping, Z.; Long, Y.; Hirata, Y. *Mater Res Innovations* 2001, 5, 101.
35. Aranguren, M. I. *Polymer* 1998, 39, 4897.
36. Nguyen, Q. T.; Bendjama, Z.; Clement, R.; Ping, Z. H. *Phys Chem Chem Phys* 1999, 1, 2761.
37. Chen, J.; Li, J. D.; Lin, Y. Z.; Chen, C. X. *J Appl Polym Sci* 2009, 112, 2425.
38. Adoor, S. G.; Prathab, B.; Manjeshwar, L. S.; Aminabhavi, T. M. *Polymer* 2007, 48, 5417.
39. Varghese, J. G.; Kittur, A. A.; Kariduraganavar, M. Y. *J Appl Polym Sci* 2009, 111, 2408.
40. Huang, Z.; Guan, H.-m.; Tan, W. I.; Qiao, X.-Y.; Kulprathi-panja, S. *J Membr Sci* 2006, 276, 260.
41. Zhang, W. D.; Sun, W.; Yang, J.; Ren, Z. Q. *Appl Biochem Biotechnol* 2010, 160, 156.
42. Shaban, H. I. *Chem Eng Process Proc Intens* 1996, 35, 429.